Contemporary Mathematics
https://ojs.wiserpub.com/index.php/CM/

Research Article

Improving Golden Jackal Optimization Algorithm Based on Elite Opposition-Based Learning: A Case Study on Breast Cancer Histopathology Images Classification

Aiedh Mrisi Alharthi[1*], Muhammad Hilal Alkhudaydi[2], Zakariya Yahya Algamal[3]

[1] Department of Mathematics, Turabah University College, Taif University, Taif, Saudi Arabia
[2] Department of Mathematics and Statistics, College of Science, Taif University, Taif, Saudi Arabia
[3] Department of Statistics and Informatics, University of Mosul, Mosul, Iraq
E-mail: amharthi@tu.edu.sa

Received: 12 June 2025; **Revised:** 11 August 2025; **Accepted:** 12 August 2025

Abstract: Feature extraction and categorization of histopathological images are crucial for predicting and diagnosing diseases such as breast cancer. A common problem with the characteristic matrix is that it includes information that is unrelated to the context. The selection of relevant characteristics has been shown to improve the efficacy of multiple categorization methods substantially. The Metaheuristic algorithm "Golden Jackal Optimization" (GJO) effectively emulates the cooperative hunting strategy of jackals. Nonetheless, it is susceptible to converging on a local optimum, since the prey's position update mostly depends on the male golden jackal, and there is a lack of diversity among golden jackals in certain situations. The Elite Opposition-Based Learning (EOBL) technique enhances the distribution of initiated solutions throughout the search space. Furthermore, the use of the EOBL method improves the algorithm's computational precision and expedites its convergence rate. The objective of this study is to enhance the efficacy of the GJO algorithm by utilizing the EOBL to improve the classification accuracy of histological images of breast cancer. Experimental results using publicly available breast cancer histopathology image datasets show that the proposed approach substantially surpasses competing algorithms in terms of overall Accuracy, Precision, Recall, and F1-score metrics. The implemented approach proved beneficial for medical picture categorization in actual clinical settings.

Keywords: golden jackal optimization, elite opposition-based learning, breast cancer, histopathology images, classification

MSC: 62F07, 68U10, 92C55

1. Introduction

Breast cancer is one of the leading causes of mortality from cancer worldwide, as reported by the World Health Organization (WHO) [1]. On the other hand, early diagnosis has been shown to boost survival rates [2]. Moreover, there are several noninvasive imaging techniques, including mammograms (X-rays), Magnetic Resonance Imaging (MRI), and ultrasonography [3, 4]. Histopathological image analysis has emerged as a significant research challenge in the field of medical imaging in recent years [5]. The diagnosis of breast cancer produced from a histopathological picture is

DOI: https://doi.org/10.37256/cm.6520257444

regarded as the "gold standard" in diagnostics since it may limit borderline diagnoses obtained from conventional imaging techniques [6].

Furthermore, the techniques of machine learning have been implemented into a computer-aided system, which has allowed for their use to boost the detection accuracy of breast cancer in women [7]. The taxonomy of normal and aberrant cellular patterns in breast cancer is one of the most fundamental and critical procedures in cancer diagnosis and treatment development [8]. The high predictive value of cancer has considerable importance in the treatment or therapy since it may aid in patient health and well-being [9].

Researchers in numerous domains, including but not limited to big data, data mining, data science, and others, have encountered severe challenges due to the explosion in data volume and feature dimensionality in recent years. It is well-known that dimensionality, sparsity, and complexity issues arise in analyzing high-dimensional data [10–12]. In addition, the classification accuracy and computational cost of machine learning classifiers also suffer when dealing with high-dimensional data. The fundamental cause of these problems is a recent rise in the number of features in the domain, from the tens to the thousands [13]. As a result, it is essential to use a feature selection strategy in order to prune the feature set. The feature selection method successfully cleans the dataset of irrelevant and distracting information. Therefore, machine learning often uses feature selection to pick the most informative subset of features while working with high-dimensional information [14]. Feature selection has been put to use in a wide variety of different domains, including but not limited to security systems, sentiment analysis, illness detection and classification, data mining, text classification, and many others [15–18].

The phenomenon of a biological population, physical sensations, the evolutionary law, and other such things inspire the development of metaheuristic algorithms, which are used to identify the best solution or a suitable solution to complicated optimization problems [19, 20]. For instance, the Whale Optimization Algorithm (WOA) was conceptualized after observing the foraging behavior of humpback whales in their natural habitat [21]. The swarming conduct of salps as they navigate and hunt for food in seas inspired the Salp Swarm Algorithm (SSA), which was developed by Mirjalili et al. [22]. The diverse processes of Harris's hawk's method for catching prey, which was introduced by Heidari et al. [23], served as the inspiration for Harris's Hawk Optimization (HHO), also known as "Harris's hawk". These algorithms get their inspiration from biological populations. For instance, control volume mass balance models that estimate both dynamic and equilibrium states served as the basis for the Equilibrium Optimizer (EO) [24]. Furthermore, Metaheuristic algorithms find widespread use in a variety of fields, including signal processing [25], image processing [26, 27], production scheduling [28], feature selection [29, 30], route planning [31], and other related fields [32–37].

Besides et al. [38] presented the strategy of Elite Opposition-Based Learning (EOBL) with the intention of improving the quality of Opposition-Based Learning (OBL). The essential purpose of EOBL is to come up with more promising solutions by analyzing the solutions that are the exact opposite of elite solutions. The alternative solution has a greater chance of situating itself in a position that is superior to the one in which the global optimum is found. The EOBL technique has been utilized to enhance the performance of meta-heuristic optimization algorithms. Furthermore, Wu et al. [39] employed EOBL during the initialization phase of Water Wave Optimization (WWO) in order to improve the convergence speed and accuracy of computation. In a similar vein, the Spider Optimization Algorithm (SOA) employed in the research conducted by Zhao et al. [40] makes use of EOBL in order to increase its computational correctness and pace of convergence. Additionally, in the study that was conducted by Huang et al. [41], they used the EOBL technique to improve the Cuckoo Search Algorithm's (CSA) capacity to strike a balance between exploratory and exploitative capabilities. Moreover, Zhang et al. [42] used EOBL to circumvent the shortcomings of the Grey Wolf Optimizer (GWO), which included a low population diversity and a sluggish convergence rate. In addition, Zhou et al. [43] used EOBL to increase the population's variety and used the greedy method to increase the Flower Pollination Algorithm's (FPA) capacity to utilize its resources. Similarly, in the study that was carried out by Tubishat et al. [44], who enhanced the Whale Optimization Algorithm (WOA) and applied it to the process of feature selection. They enhanced the exploitation phase of the algorithm by introducing an advanced local search, and they improved the exploration stage of the algorithm by implementing the EOBL method.

Recently, the cooperative hunting behaviors of golden jackals provided the basis for a new biological swarm intelligence algorithm that was introduced by Chopra and Mohsin [45]. This method is known as the Golden Jackal

Optimization (GJO) algorithm. Even though it is simple to build, has a high level of stability, and requires only a small number of adjustment parameters, the GJO algorithm has imbalanced exploration and exploitation capabilities. This may easily result in excessive exploitation and a collapse into a local optimal state. Whenever there is an iteration taking place, the location of the prey will always be situated in the midst of the two golden jackals. However, the site of male golden jackals is not always the ideal option. This may easily lead to delayed convergence in the late iterations, poor convergence precision, and the easy occurrence of slipping into a locally optimal solution.

Moreover, Houssein et al. [46] presented an opposition-based golden jackal optimization technique to tackle the multilevel thresholding issue, using Otsu's approach as the objective function. The results indicate that the proposed technique surpasses the performance of the other seven meta-heuristic techniques and effectively resolves the segmentation issue. Furthermore, Rezaie et al. [47] proposed a methodology to ascertain the optimal characteristics of Proton Exchange Membrane Fuel Cells (PEMFCs). The methodology used a customized variant of the Golden Jackal Optimization technique to minimize the Sum of Squared Errors (SSE) among the model's output voltages and the observed data. The results indicate that the proposed method outperforms previous comparative methods in accurately estimating the optimal value of the PEMFC model. Mohapatra and Mohapatra [48] introduced a computational procedure called the Fast Random Opposition-Based Learning Golden Jackal Optimization (FROBL-GJO) method. The results suggest that the FROBL-GJO method outperforms other well-recognized meta-heuristic algorithms in solving engineering design and global optimization challenges. Additionally, Devi et al. [49] introduced an enhanced version of theGolden Jackel Optimization Algorithm (GJOA) that incorporates a local escape operator and considers the direction of population movement. These modifications aim to increase the algorithm's capacity to explore and utilize the search space. The results suggest that the revised GJO is a viable method for addressing feature selection and numerical optimization problems. Alharthi et al. [50] proposed an enhancement to the GJO method that uses chaotic maps. This development aims to increase the GJO algorithm's exploration and exploitation capabilities in selecting the crucial descriptors in Quantitative Structure-Activity Relationship (QSAR) classification models while simultaneously reducing the computing time required.

In view of that, optimization strategies are necessary in several study disciplines to find optimal solutions to complex problems. The GJO and EOBL methods have been used in several research fields to address their issues. Thus, when combined, EOBL and GJO complement each other in the following ways. Firstly, EOBL provides a strong exploration capability, allowing the algorithm to cover a wide range of the search space efficiently. This is particularly beneficial for GJO ensures that the algorithm does not get stuck in local optima and can effectively explore diverse regions of the search space. Secondly, GJO's cooperative hunting and local search strategies enhance the exploitation capabilities of EOBL. By focusing on the promising regions that EOBL identifies, GJO can intensively explore these areas, fine-tune the solutions, and converge towards the global optimum. This combination of exploration (EOBL) and exploitation (GJO) strategies allow for a more balanced and effective optimization process. Therefore, this study focuses on improving the performance of the GJO algorithm using the EOBL, abbreviated as EOBL-GJO, to increase the classification accuracy of the histopathological images of breast cancer and address the shortcomings of the GJO algorithm. Experimental results based on publicly available breast cancer histopathological image datasets showed that the proposed method significantly outperforms other competitor methods regarding Accuracy, Precision, Recall, and F1-score criteria and computational time to improve the classification accuracy of the histopathological images of breast cancer. The rest of the current paper is organized as follows: Section 2 covers the details of the GJO and EOBL algorithms and our proposed method. The experimental study is presented in Section 3. Section 4 discusses and summarizes the findings. Section 5 provides a conclusion.

2. Methods

2.1 *GJOA*

Chopra and Ansari presented the Golden Jackal Optimization (GJO) algorithm as a swarm intelligence technique [45]. For the purpose of hunting, this program makes an effort to mimic the actions of wild golden jackals. Golden jackals,

both sexes, often go hunting together. There are three main steps to a golden jackal's hunting process: (1) scouting for potential prey and advancing toward it, (2) encircling and frightening the prey until it stops moving, and (3) pouncing on the victim. The search space is randomly distributed with a population of golden jackals in the Golden Jackal algorithm. Next, a set of rules that mimics jackals' hunting and foraging behaviour is used to repeatedly change the locations of these golden jackals. According to [45, 51], the fitness values of each golden jackal in the population are utilized to ascertain how the population's "best" golden jackal should be updated. Following this, the mathematical model of the GJO method will be displayed.

2.1.1 *Search model*

The following matrix can be used to specify the prey's random placement during the procedure's first phase [45, 52]:

$$\begin{bmatrix} Y_{1,\,1} & Y_{1,\,2} & \cdots & \cdots & Y_{1,\,n} \\ Y_{2,\,1} & Y_{2,\,2} & \cdots & \cdots & Y_{2,\,n} \\ \vdots & \vdots & \vdots & \vdots & \vdots \\ \vdots & \vdots & \vdots & \vdots & \vdots \\ Y_{N,\,1} & Y_{N,\,2} & \cdots & \cdots & Y_{N,\,n} \end{bmatrix} \tag{1}$$

here, N denotes the overall count of prey populations, whereas n represents the number of dimensions in the region under consideration.

2.1.2 *Exploration phase*

Capturing prey is challenging due to jackals' inherent ability to track their prey. Consequently, jackals will hide in the vicinity to capture other prey. The hunting behaviour can be mathematically described as $(|E| > 1)$ [49, 53]:

$$Y_1(t) = Y_M(t) - E \cdot |Y_M(t) - rl \cdot Prey(t)| \tag{2}$$

$$Y_2(t) = Y_{FM}(t) - E \cdot |Y_{FM}(t) - rl \cdot Prey(t)| \tag{3}$$

where, $Y_M(t)$ and $Y_{FM}(t)$ indicate the locations of the male and female jackals, respectively, and is the present algorithm iteration. $Prey(t)$ is a vector representing the hunting position, whereas $Y_1(t)$ and $Y_2(t)$ are functions that, when changed, indicate the updated location of the jackals. Below is the formula for the prey's escape energy, abbreviated as "E" [51, 53]

$$E = E_1 \cdot E_0 \tag{4}$$

$$E_0 = 2 \cdot r - 1| \tag{5}$$

$$E_1 = c_1 \cdot \left(1 - \left(\frac{t}{T}\right)\right) \tag{6}$$

here, E_0 is the initial energy of the prey, which may take on a value between -1 and 1; T is the maximum number of repeats, c_1 is a constant that is initially set to 1.5, $0 < r < 1$, and E_1 denotes the prey's declining energy. In Eq. (4), they interact multiplicatively, meaning both must be considered to determine EE. Their interaction is straightforward but

essential in determining the effect one factor's value has on the overall product within the system or model where this equation applies. The jackal's distance from its prey is represented by $|Y_M(t) - (rl) \cdot Prey(t)|$ as Eqs. (2) and (3). The formula for calculating "*rl*", a vector of random values produced via the Levy Flight (LF) function is stated in [49, 53]:

$$rl = (5) \cdot \frac{LF(y)}{100} \tag{7}$$

where,

$$LF(y) = \frac{(\mu) \cdot (\sigma)}{(100) \cdot \left| \upsilon^{\left(\frac{1}{\beta}\right)} \right|}, \quad \sigma = \left(\frac{\Gamma(1+\beta) \cdot sin\left(\frac{\pi\beta}{2}\right)}{\Gamma\left(\frac{1+\beta}{2}\right) \cdot (\beta) \cdot (2^{\beta-1})} \right)^{\frac{1}{\beta}} \tag{8}$$

here, v is a randomly generated integer ranging from 0 to 1, Γ is the gamma function, is the amount of the second part, and β is a constant value that is supposed to be 1.5 [49].

$$Y(t+1) = \frac{Y_1(t) + Y_2(t)}{2} \tag{9}$$

In Eq. (9), $Y(t+1)$ represents the prey's most recent location with respect to the jackals and it simplifies calculations and analysis, reducing potential bias toward either input [53].

2.1.3 *Exploitation phase*

During the procedure, the mysterious energy of the prey reduces as jackals pursue it. This ultimately results in the prey being encircled by a pair of jackals that were discovered sooner in the process. Following the victim's encirclement, the jackals will attack it and then consume it in the end. The following mathematical model represents the behaviour of both male and female jackals at the same time as they hunt together ($|E| \leq 1$) [54, 45]:

$$Y_1(t) = Y_M(t) - E \cdot |rl \cdot Y_M(t) - Prey(t)| \tag{10}$$

$$Y_2(t) = Y_{FM}(t) - E \cdot |rl \cdot Y_{FM}(t) - Prey(t)| \tag{11}$$

Eqs. (10) and (11) use *rl* to allow for random behaviour during the exploitation stage, which encourages exploration and prevents local optima, and it produced vector updates. Exploration and exploitation are balanced out by the energy that the prey requires to escape. As it tries to outrun its attacker, the prey's remaining energy drops rapidly. The initial energy, E_0, may take on a value between -1 and 1 at random in each cycle of the loop. A decrease in E_0, from 0 to -1 makes the prey more susceptible to harm, whereas an increase from 0 to 1 makes it more resistant. The jackal duo will explore different regions for potential prey while $|E| \geq 1$, but when $|E| < 1$, they will attack and take advantage of their victim [51, 53]. The GJO algorithm's pseudo-code is shown in Algorithm 1 [45, 49, 52].

2.2 *EOBL*

Tizhoosh first presented the OBL approach [55], and the EOBL technique is an upgraded version of that technique [38]. The OBL approach is a method of machine intelligence that was developed with the purpose of enhancing the efficiency of optimization algorithms. This method takes into account the possibility of finding a more advantageous solution among the existing persons, which is often initiated in a random fashion by the optimization algorithm, as well as the solution that corresponds to the opposite outcome. In both of the solutions, the evaluation function is used, and the solution that is deemed to be the superior one is chosen for the subsequent iteration.

Algorithm 1 Pseudo-code for the GJO

1: **Inputs:** The size of the population, "N", and maximal iteration count, "T".
2: **Outputs:** The prey's location and worth as a fit prey.
3: Create a random prey population, $(Y_i,\ i = 1,\ 2,\ ...,\ N)$.
4: **while** $(t < T)$ **do**
5: Compute the prey's fitness values
6: Y_1 = Best prey (Male Jackal Position)
7: Y_2 = Secondbest prey (Female Jackal Position)
8: **for** (**do** every prey)
9: Update the evading energy "E" by Eqs. (4), (5), and (6)
10: Update "rl" by Eqs. (7) and (8)
11: **if** $(|E|1)$ **then**
12: Update the prey position by Eqs. (2), (3), and (9)
13: **end if**
14: **if** $(|E| > 1)$ **then**
15: Update the prey position by Eqs. (9), (10), and (11)
16: **end if**
17: $t = t + 1$
18: **end for**
19: **end while**
20: **Return** Y_1

A mathematical model of OBL may be constructed as follows: In the current population, let $x = (x_1,\ x_2,\ ...,\ x_D)$ represents a point. D represents the problem of dimensional space and $x \in [a_i,\ b_i]$, where $i = 1,\ 2,\ ...,\ D$. The opposition point $\breve{x} = (\breve{x}_1,\ \breve{x}_2,\ ...,\ \breve{x}_D)$ may therefore be described by the equation that follows [56]:

$$\breve{x}_i = a_i + b_i - x_i \tag{12}$$

The EOBL utilizes an exceptional person to guide the populace toward the global ideal answer. The elite person is more likely to possess useful knowledge than others. Essentially, EOBL employs the elite person in the present population to develop equivalent opposites of the existing particles inside the search dimension. Thus, the elite will direct the particles till they reach a potential place where the best answer may be discovered. As a result, using the EOBL approach will increase population variety while also improving GJO algorithm exploration. As indicated, EOBL was previously used in the literature to enhance numerous optimization techniques [57–59].

The present study uses the EOBL method to improve the exploration ability of GJO algorithms. As an alternative position, the following is one possible expression: for the individual $X_i = (x_{i,\ 1},\ x_{i,\ 2},\ ...,\ x_{i,\ D})$ in the current population $X_e = (x_{e,\ 1},\ x_{e,\ 2},\ ...,\ x_{e,\ D})$; therefore, the elite opposite position can be $\breve{X}_i = (\breve{x}_{i,\ 1},\ \breve{x}_{i,\ 2},\ ...,\ \breve{x}_{i,\ D})$ formulated as [56]

$$\breve{x}_{i,\ j} = S \times (da_j + db_j) - x_{i,\ j} \tag{13}$$

where $S \in [0,\ 1]$ and C is a generalization factor. da_j and db_j are dynamic boundaries, which are formulated as

$$da_j = min(x_{i,\ j}), \quad db_j = max(x_{i,\ j}) \tag{14}$$

where min and max are the minimum and the maximum of the value. That being said, the search boundaries $[a_i,\ b_i]$ may not encompass the inverse outcome. As a solution to this problem, the transferred person is given a random value between, denoted as [57]

$$\check{x}_{i,\ j} = rand(a_j,\ b_j),\ \text{if}\ \check{x}_{i,\ j} < a_j || \check{x}_{i,\ j} > b_j \tag{15}$$

The generation of a separate population from opposing solutions is how EOBL manages to promote population variety. Varying amounts of randomness during the search can balance exploration and exploitation, leading to better and potentially faster convergence. In light of this, the GJO's capacity for exploration has been enhanced.

2.2.1 *Proposed algorithml*

Population initialization is a non-repeatable process; however, the results of other stages can be derived from it. Whenever the quality of the initial population has to be initialized as per the nature of the problem, it becomes very important. The smoothness of convergence of GJO, in particular, as the general picture of its work, the time taken to arrive at a final solution, and the reliability of the solution. Starting from the original GJO, such initialisation schemes have been used for various GJOs. The idea was to see if the first population generated from the given adjoining matrix could be more evenly distributed across the search space, free from local or sub-optimal solution traps.

By foregrounding the representativeness of oppositeness, the solution space is dichotomized. These disciplines are then applied over the regions so that benefit may be gained about the solution space. EOBL can further search the GJO algorithm's search space, that is, search for a larger area of better potential solutions in an optimal approach, which enhances the solution search process. Subsequently, preserving the opposite of this within the search space increases the differentiation in the use of the search and helps to prevent jumping into a local optimum.

In this section, the GJO algorithm's structure is described in detail to enhance the performance of the proposed model. At this point, the original composition of the GJO is adjusted by adding the EOBL approach to supplement and complement the deficiencies in the GJO, such as the ability to delve into the search domain or quickly converge to the best value. The proposed algorithm, EOBL-GJO, improves the GJO algorithm through two stages: In the first place, EOBL is employed for the purpose of initializing the population in order to increase the rate of convergence and also to prevent the GJO algorithm avoids being trapped in a local optimum by searching the solutions in the entire domain of the search space. Secondly, the position of the golden jackals has been updated according to one prominent conventional GJO strategy. The EOBL is also utilized to decide whether the value of the fitness function of the opposite solution is better than that of the new solution.

In the first stage, the initial population is randomly generated. Then, the elite opposite positions are obtained by the EOBL (Eq. (13)), and they are used to construct the opposite population. Thus, in the second stage, we update the positions of golden jackals by applying steps of the original GJO algorithm and then apply the EOBL technique to produce the set of elite opponent's positions. After that, the EOBL-GJO constructs the new population by selecting the best current population and the opposite population based on fitness function values.

The convergence rate of GJO depends on various factors, including the problem complexity, parameter settings, and initial population. In GJO, the random numbers control the exploration and exploitation abilities of the algorithm. A balance between these parameters is crucial. In addition, the convergence rate of GJO will depend on the parameter setting of the used classifier. On the other hand, the time complexity of GJO is $O(t \times n) + O(t \times n \times d)$. This process is briefly described in Figure 1.

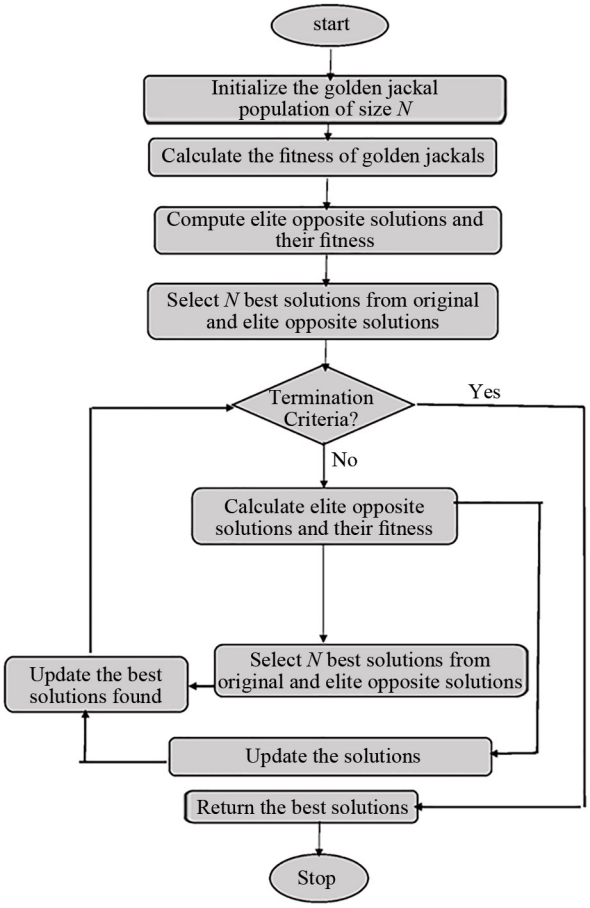

Figure 1. Flowchart of the EOBL-GJO algorithm

3. Experimental study

3.1 *Datasets description*

This study utilizes a Breast Histopathology (BH) dataset that is available to the public on Kaggle [60]. The number 36. The dataset comprises 277,524 images obtained from 179 patients. These patients are classified as either Invasive Ductal Carcinoma (IDC) positive or IDC negative. The total count of cancer patches that test positive for IDC is 78,786, indicating malignancy. Conversely, there are 198,738 negative images. The collection comprises Portable Network Graphics (PNG) images with dimensions of 50 × 50 pixels, scanned at 40 × resolution. Approximately 265,142 samples for training and 128,382 for testing, though splits vary among studies and sometimes use cross-validation. Figure 2 exhibits both malignant and benign samples from this collection of data [61].

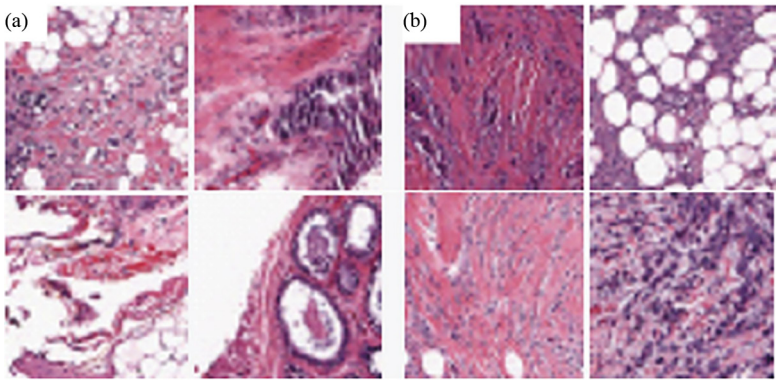

Figure 2. Ataset samples (a) Non-cancerous, (b) Cancerous

3.2 *Performance evaluation*

Four different metrics for the assessment of performance measures are used for our proposed algorithm. It measures the quality of the classification made by the classification models when they classify the test data and gives the performance of the classifier. Out of all the metrics prevalent in classification, the relevant metrics for our purpose are Accuracy, Precision, Recall, and F1-score. Accuracy goes along the line of the precision metric, where we measure how many of the classes that we predicted are actually correct in relation to the total number of classes that we have predicted. Accuracy calculates the number of instances in which the classifier is right on the positive classes over the total number of positive classes as classified by the classifier. Recall is one of a model's measures, which is an expression of the correctly supposed number of positive classes to the actual number of positive classes. F1-score uses both precision and recall.

$$\text{Accuracy} = \frac{\text{TP}+\text{TN}}{\text{TP}+\text{TN}+\text{FP}+\text{FN}} \tag{16}$$

$$\text{Precision} = \frac{\text{TP}}{\text{TP}+\text{FP}} \tag{17}$$

$$\text{Recall} = \frac{\text{TP}}{\text{TP}+\text{FN}} \tag{18}$$

$$\text{F1-score} = \frac{2(\text{Recall}\times\text{Prescision})}{(\text{Recall}+\text{Prescision})} \tag{19}$$

where TP is the true positives, TN is the true negatives, FP is the false positives, and FN is the false negatives.

3.3 *Experimental setting*

The classification procedure will predict whether the histopathology image is a benign one or a malignant one. Three classifiers are used in this study: Support Vector Machine (SVM) with radial basis kernel, k-Nearest Neighbor (k-NN) with $k = 5$, and Random Forest (RF). The dataset is divided into two categories: training 80% and testing 20% of data. This splitting is performed on 20 runs, and the average performance evaluation is computed for each algorithm used.

4. Result and discussion

When EOBL is integrated with the GJO algorithm, it can significantly improve the performance of breast cancer histopathology image classification. This can be shown by accelerating convergence since the EOBL will introduce a new population of solutions. Further, EOBL-GJO can improve the balance between the exploration and the exploitation of GJO to avoid local optima and to find global solutions. As a result, the classification accuracy of the breast cancer histopathology image will be enhanced. This is because EOBL can help GJO identify more relevant features from histopathology images, leading to better classification performance.

The performance of the proposed procedure, EOBL-GJO, is compared with the opposition-based learning, OBL-GJO, and the standard GJO algorithm. The performance evaluation of the used algorithms for training and test data and for the three classifiers is provided in Tables 1-6, respectively. The highest classification performance is indicated in bold. In addition, the standard deviation values are also provided for each of the performance evaluation criteria.

From Tables 1, 3, and 5, in terms of the Accuracy criterion, regardless of the type of classifier, we can see that EOBL-GJO achieves the highest average classification accuracy in classifying cancer images as benign or malignant. For example, from Table 3, the classification accuracy using EOBL-GJO increased by 3.154% and 1.577% compared with GJO and OBL-GJO, respectively. Simultaneously, in terms of Precision, Recall, and F1-score criteria, our proposed approach, EOBL-GJO, obtains excellent performance in the training data for all the types of classifiers. It is evident that the EOBL-GJO achieved the highest results, while OBL-GJO and GJO ranked second and third, respectively.

By reading the results depending on the test data from Tables 2, 4, and 6, once again, we can observe that our proposed approach, EOBL-GJO, still exhibits higher average classification accuracy than OBL-GJO and GJO, indicating that EOBL-GJO outperforms both OBL-GJO and GJO algorithms. Furthermore, in terms of Precision, Recall, and F1-score criteria, EOBL-GJO gives superior results compared to OBL-GJO and GJO algorithms. It is inferred from Tables 2, 4, and 6 that the average Precision criterion of the EOBL-GJO, regardless of the classifier type, is 0.943. In other words, 94.3% of cancer images are classified as benign classification by EOBL-GJO among the entire datasets. The average Recall value of the EOBL-GJO is 0.944, i.e., 94.4% of benign cases are classified correctly with positive results by EOBL-GJO. Additionally, the average F1-score of the EOBL-GJO is 0.943, i.e., 94.3% of wrongly classified cases are identified correctly by EOBL-GJO.

Regarding the standard deviation results of Tables 1-6, EOBL-GJO is stable, generating low standard deviation values compared to both OBL-GJO and GJO algorithms. Moreover, regarding the type of classifiers, in general, it is clear that SVM outperformed KNN and RF in terms of Accuracy, Precision, Recall, and F1-score criteria using EOBL-GJO, OBL-GJO and GJO algorithms. EOBL-GJO gives superior outcomes, while the conventional GJO algorithm has lower performance in classifying cancer images as benign or malignant.

Table 1. Average performance valuation of the algorithm used for the training data based on the KNN classifier

	GJO	OBL-GJO	EOBL-GJO
Accuracy	0.912 ± 0.021	0.927 ± 0.017	0.941 ± 0.014
Precision	0.914 ± 0.020	0.931 ± 0.018	0.945 ± 0.015
Recall	0.917 ± 0.021	0.934 ± 0.017	0.947 ± 0.015
F1-score	0.915 ± 0.021	0.932 ± 0.017	0.945 ± 0.015

Table 2. Average performance valuation of the used algorithm for the testing data based on the KNN classifier

	GJO	BL-GJO	EOBL-GJO
Accuracy	0.905 ± 0.023	0.921 ± 0.020	0.934 ± 0.018
Precision	0.907 ± 0.022	0.924 ± 0.020	0.938 ± 0.018
Recall	0.912 ± 0.021	0.927± 0.022	0.941 ± 0.017
F1-score	0.908 ± 0.021	0.925 ± 0.021	0.938 ± 0.017

Table 3. Average performance valuation of the used algorithm for the training data based on the SVM classifier

	GJO	BL-GJO	EOBL-GJO
Accuracy	0.921 ± 0.018	0.936 ± 0.016	0.951 ± 0.014
Precision	0.923 ± 0.018	0.942 ± 0.015	0.954 ± 0.014
Recall	0.926 ± 0.019	0.943 ± 0.016	0.956 ± 0.014
F1-score	0.924 ± 0.018	0.941 ± 0.016	0.954 ± 0.014

Table 4. Average performance valuation of the used algorithm for the testing data based on the SVM classifier

	GJO	BL-GJO	EOBL-GJO
Accuracy	0.915 ± 0.019	0.932 ± 0.017	0.944 ± 0.015
Precision	0.917 ± 0.019	0.934 ± 0.016	0.948 ± 0.015
Recall	0.921 ± 0.018	0.937 ± 0.016	0.952 ± 0.014
F1-score	0.918 ± 0.018	0.935 ± 0.016	0.948 ± 0.015

Table 5. Average performance valuation of the algorithm used for the training data based on the RF classifier

	GJO	BL-GJO	EOBL-GJO
Accuracy	0.917 ± 0.021	0.932 ± 0.018	0.946 ± 0.017
Precision	0.919 ± 0.020	0.936 ± 0.017	0.953 ± 0.018
Recall	0.922 ± 0.020	0.939 ± 0.018	0.952 ± 0.016
F1-score	0.921 ± 0.020	0.937 ± 0.018	0.951 ± 0.017

Table 6. Average performance valuation of the used algorithm for the testing data based on the RF classifier

	GJO	BL-GJO	EOBL-GJO
Accuracy	0.911 ± 0.022	0.926 ± 0.020	0.941 ± 0.019
Precision	0.913 ± 0.020	0.932 ± 0.019	0.944 ± 0.020
Recall	0.916 ± 0.021	0.933 ± 0.020	0.946 ± 0.019
F1-score	0.914 ± 0.021	0.931 ± 0.020	0.944 ± 0.020

Figure 3 compares the computational time in seconds to further highlight the performance of the proposed approach, EOBL-GJO. The results show that EOBL-GJO requires less computational time than GJO algorithms. EOBL-GJO

exhibits a slightly faster training speed than OBL-GJO. As a consequence, EOBL-GJO is considerably faster than OBL-GJO and GJO.

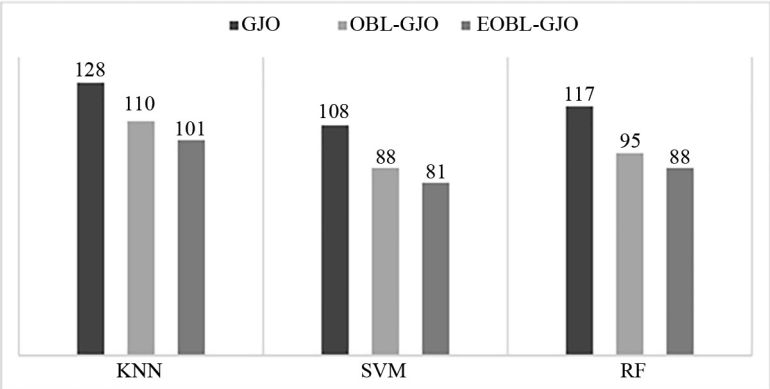

Figure 3. Average computational time in seconds for the used algorithms

In order to verify the significance of the obtained results in terms of F1-score, the Wilcoxon signed-rank test, which is a nonparametric statistical test, is carried out. This test compares the performance of the proposed approach, EOBL-GJO, with that of the OBL-GJO and GJO algorithms. In this test, the null hypothesis, which states that there is no significant difference between the EOBL-GJO and each one of the OBL-GJO and GJO algorithms, is tested against the alternative hypothesis, which states that there is a significant difference between the EOBL-GJO and each of the OBL-GJO and GJO. According to the statistical value, the null hypothesis is accepted if this statistical value is greater than 0.05; otherwise, the alternative hypothesis is accepted. Table 7 shows the *p*-values of the Wilcoxon signed-rank test results between the EOBL-GJO, OBL-GJO, and GJO algorithms along each classifier. In the table, the *p*-values are marked with "S" which indicates that there is a significant difference between the EOBL-GJO and the other algorithms. *p*-values marked with "NS" indicate that there is no statistical difference between the EOBL-GJO and the comparison algorithm. From Table 7, it can be observed that there is a significant difference between the EOBL-GJO algorithm and the others on all the classifiers.

Table 7. The results of Wilcoxon's rank sum test using the average F1-score

EOBL-GJO vs	OBL-GJO	GJO
KNN	0.0241 "S"	0.0043 "S"
SVM	0.0173 "S"	0.0029 "S"
RF	0.0211 "S"	0.0035 "S"

Based on the result and discussion of this work, it can be concluded that the scheme using elite opposition-based learning is effective and has a positive impact on enhancing the GJO algorithm performance. The procedure for creating the first population in the GJO can affect the function of the GJO in a way that is best for the algorithm. It is revealed that the proposed method has high potential for identifying an appropriate initial population thanks to the EOBL, which explores large areas of the search domain and avoids creating identical solutions. This results in the simultaneous production of numerous solutions across the entire optimization process and enhanced localization of the local optima, which are the two key factors that make the proposed technique favorable for classifying histopathology cancer images as either benign or malignant.

To further evaluate the performance of the proposed EOBL-GJO algorithm, four optimization algorithms have been selected and compared with EOBL-GJO. Table 8 gives the comparative results between EOBL-GJO and Particle Swarm

Optimization (PSO), Coyote Optimization Algorithm (COA), Bat Algorithm (BA), Sine Cosine Algorithm (SCA), and Grey Wolf Optimization (GWO). Based on the results reported in Table 8, it can be concluded that EOBL-GJO provided the best results regarding Accuracy, Precision, Recall, and F1-score criteria.

Table 8. Average performance among state-of-the-art algorithms used for the training data based on the SVM classifier

	PSO	COA	SCA	EOBL-GJO
Accuracy	0.904 ± 0.023	0.914 ± 0.020	0.927 ± 0.017	0.946 ± 0.017
Precision	0.908 ± 0.022	0.919 ± 0.021	0.930 ± 0.020	0.953 ± 0.018
Recall	0.910 ± 0.022	0.923 ± 0.021	0.941 ± 0.018	0.952 ± 0.016
F1-score	0.912 ± 0.023	0.928 ± 0.021	0.944 ± 0.019	0.951 ± 0.017

5. Conclusion

The process of classifying breast cancer is widely regarded as an important one in the field of medicine. In this article, we presented the GJO-EOBL algorithm, which has shown good results in terms of enhancing the performance of the GJO Algorithm and, as a result, raises the classification accuracy of the histopathological images used for breast cancer diagnosis. Our suggested method has been shown to have superior performance in terms of accuracy, precision, recall, and F1-score when compared to both the OBL-GJO and GJO algorithms, as evidenced by the experimental findings and statistical analysis conducted on the Breast Histology (BH) dataset. This shows that our proposed algorithm is superior to both of these algorithms. When it comes to expressing the data connection between the input features and target variables, the GJO-EOBL is thus more appropriate than the other models. Through the use of these techniques, there is the potential to enhance the detection and treatment of breast cancer, which would ultimately result in better outcomes for patients. Several different real-world applications can make use of this very successful predictive architecture.

Acknowledgement

The authors would like to acknowledge the Deanship of Graduate Studies and Scientific Research, Taif University, for funding this work through project number (202310).

Conflict of interest

The authors declare no competing financial interest.

References

[1] Kadam VJ, Jadhav SM, Vijayakumar K. Breast cancer diagnosis using feature ensemble learning based on stacked sparse autoencoders and softmax regression. *Journal of Medical Systems*. 2019; 43(8): 263. Available from: https://doi.org/10.1007/s10916-019-1397-z.

[2] Sheikhpour R, Sarram MA, Sheikhpour R. Particle swarm optimization for bandwidth determination and feature selection of kernel density estimation based classifiers in diagnosis of breast cancer. *Applied Soft Computing*. 2016; 40: 113-131. Available from: https://doi.org/10.1016/j.asoc.2015.10.005.

[3] Acharya UR, Raghavendra U, Fujita H, Hagiwara Y, Koh JE, Jen Hong T, et al. Automated characterization of fatty liver disease and cirrhosis using curvelet transform and entropy features extracted from ultrasound images. *Computers in Biology and Medicine*. 2016; 79: 250-258. Available from: https://doi.org/10.1016/j.compbiomed.2016.10.022.

[4] Spanhol FA, Oliveira LS, Petitjean C, Heutte L. A dataset for breast cancer histopathological image classification. *IEEE Transactions on Biomedical Engineering*. 2016; 63(7): 1455-1462. Available from: https://doi.org/10.1109/TBME.2015.2496264.

[5] Zhang Y, Zhang B, Lu W. Breast cancer classification from histological images with multiple features and random subspace classifier ensemble. *AIP Conference Proceedings*. 2011; 1371(1): 19-28. Available from: https://doi.org/10.1063/1.3596623.

[6] Vu TH, Mousavi HS, Monga V, Rao G, Rao UKA. Histopathological image classification using discriminative feature-oriented dictionary learning. *IEEE Transactions on Medical Imaging*. 2016; 35(3): 738-751. Available from: https://doi.org/10.1109/TMI.2015.2493530.

[7] Belsare AD, Mushrif MM, Pangarkar MA, Meshram N. Classification of breast cancer histopathology images using texture feature analysis. In: *TENCON 2015-2015 IEEE Region 10 Conference*. Macao, China: IEEE; 2016. Available from: https://doi.org/10.1109/TENCON.2015.7372809.

[8] Korkmaz S, Zararsiz G, Goksuluk D. Drug/nondrug classification using Support Vector Machines with various feature selection strategies. *Computer Methods and Programs in Biomedicine*. 2014; 117(2): 51-60. Available from: https://doi.org/10.1016/j.cmpb.2014.08.009.

[9] Chen Y, Wang L, Li L, Zhang H, Yuan Z. Informative gene selection and the direct classification of tumors based on relative simplicity. *BMC Bioinformatics*. 2016; 17: 44. Available from: https://doi.org/10.1186/s12859-016-0893-0.

[10] Khanan A, Abdullah S, Mohamed AHHM, Mehmood A, Ariffin KAZ. Big data security and privacy concerns: A review. *Smart Technologies and Innovation for a Sustainable Future*. Heidelberg: Springer; 2019. Available from: https://doi.org/10.1007/978-3-030-01659-3_8.

[11] Algamal ZY, Lee MH, Al-Fakih AM, Aziz M. High-dimensional QSAR classification model for anti-hepatitis C virus activity of thiourea derivatives based on the sparse logistic regression model with a bridge penalty. *Journal of Chemometrics*. 2017; 31(6): e2889. Available from: https://doi.org/10.1002/cem.2889.

[12] Algamal Z, Qasim M, Ali H. A QSAR classification model for neuraminidase inhibitors of influenza A viruses (H1N1) based on weighted penalized support vector machine. *SAR and QSAR in Environmental Research*. 2017; 28(5): 415-426. Available from: https://doi.org/10.1080/1062936X.2017.1326402.

[13] Halim MA, Abdullah A, Ariffin KAZ. Recurrent neural network for malware detection. *International Journal of Advances in Soft Computing and Its Applications*. 2019; 11(1): 46-63.

[14] Arram A, Ayob M, Kendall G, Sulaiman A. Bird mating optimizer for combinatorial optimization problems. *IEEE Access*. 2020; 8: 96845-96858. Available from: https://doi.org/10.1109/ACCESS.2020.2993491.

[15] Alkahya MA, Alreahan HO, Algamal ZY. Classification of breast cancer histopathological images using adaptive penalized logistic regression with wilcoxon rank sum test. *Electronic Journal of Applied Statistical Analysis*. 2023; 16(3): 507-518.

[16] Sihwail R, Omar K, Ariffin KAZ. A survey on malware analysis techniques: Static, dynamic, hybrid and memory analysis. *International Journal on Advanced Science, Engineering and Information Technology*. 2018; 8(4-2): 1662. Available from: https://doi.org/10.18517/ijaseit.8.4-2.6827.

[17] Almishlih ZA, Qasim OS, Algamal ZY. Binary arithmetic optimization algorithm using a new transfer function for fusion modeling. *Fusion: Practice and Applications*. 2025; 18(2): 157-168. Available from: https://doi.org/10.54216/FPA.180212.

[18] Alharthi A, Kadir D, Al-Fakih A, Algamal Z, Al-Thanoon N, Qasim M. Quantitative structure-property relationship modelling for predicting retention indices of essential oils based on an improved horse herd optimization algorithm. *SAR and QSAR in Environmental Research*. 2023; 34(10): 831-846. Available from: https://doi.org/10.1080/1062936X.2023.2261855.

[19] Song PC, Chu SC, Pan JS, Yang H. Simplified Phasmatodea population evolution algorithm for optimization. *Complex and Intelligent Systems*. 2022; 8(4): 2749-2767. Available from: https://doi.org/10.1007/s40747-021-00402-0.

[20] Sun XX, Pan JS, Chu SC, Hu P, Tian AQ. A novel pigeon-inspired optimization with QUasi-Affine TRansformation evolutionary algorithm for DV-Hop in wireless sensor networks. *International Journal of Distributed Sensor Networks*. 2020; 16(6): 155014772093274. Available from: https://doi.org/10.1177/1550147720932749.

[21] Mirjalili S, Lewis A. The whale optimization algorithm. *Advances in Engineering Software*. 2016; 95: 51-67. Available from: https://doi.org/10.1016/j.advengsoft.2016.01.008.

[22] Mirjalili S, Gandomi AH, Mirjalili SZ, Saremi S, Faris H, Mirjalili SM. Salp swarm algorithm: A bio-inspired optimizer for engineering design problems. *Advances in Engineering Software*. 2017; 114: 163-191. Available from: https://doi.org/10.1016/j.advengsoft.2017.07.002.

[23] Heidari AA, Mirjalili S, Faris H, Aljarah I, Mafarja M, Chen H. Harris hawks optimization: Algorithm and applications. *Future Generation Computer Systems*. 2019; 97: 849-872. Available from: https://doi.org/10.1016/j.future.2019.02.028.

[24] Faramarzi A, Heidarinejad M, Stephens B, Mirjalili S. Equilibrium optimizer: A novel optimization algorithm. *Knowledge-Based Systems*. 2020; 191: 105190. Available from: https://doi.org/10.1016/j.knosys.2019.105190.

[25] Valayapalayam Kittusamy SR, Elhoseny M, Kathiresan S. An enhanced whale optimization algorithm for vehicular communication networks. *International Journal of Communication Systems*. 2022; 35(12): e3953. Available from: https://doi.org/10.1002/dac.3953.

[26] Guo L, Liu L, Zhao Z, Xia X. An improved RIME optimization algorithm for lung cancer image segmentation. *Computers in Biology and Medicine*. 2024; 174: 108219. Available from: https://doi.org/10.1016/j.compbiomed.2024.108219.

[27] Rather SA, Bala PS. Constriction coefficient based particle swarm optimization and gravitational search algorithm for multilevel image thresholding. *Expert Systems*. 2021; 38(7): 1-36. Available from: https://doi.org/10.1111/exsy.12717.

[28] Cao X, Yang ZY, Hong WC, Xu RZ, Wang YT. Optimizing berth-quay crane allocation considering economic factors using chaotic quantum SSA. *Applied Artificial Intelligence*. 2022; 36(1): e2073719. Available from: https://doi.org/10.1080/08839514.2022.2073719.

[29] Naik AK, Kuppili V. An embedded feature selection method based on generalized classifier neural network for cancer classification. *Computers in Biology and Medicine*. 2024; 168: 107677. Available from: https://doi.org/10.1016/j.compbiomed.2023.107677.

[30] Samieiyan B, MohammadiNasab P, Mollaei MA, Hajizadeh F, Kangavari M. Novel optimized crow search algorithm for feature selection. *Expert Systems with Applications*. 2022; 204: 117486. Available from: https://doi.org/10.1016/j.eswa.2022.117486.

[31] Phung MD, Ha QP. Safety-enhanced UAV path planning with spherical vector-based particle swarm optimization. *Applied Soft Computing*. 2021; 107: 107376. Available from: https://doi.org/10.1016/j.asoc.2021.107376.

[32] Kahya MA, Altamir SA, Algamal ZY. Improving whale optimization algorithm for feature selection with a timevarying transfer function. *Numerical Algebra, Control and Optimization*. 2020; 11(1): 87-98. Available from: https://doi.org/10.3934/naco.2020017.

[33] Ismael OM, Qasim OS, Algamal ZY. Improving Harris hawks optimization algorithm for hyperparameters estimation and feature selection in v-support vector regression based on opposition-based learning. *Journal of Chemometrics*. 2020; 34(11): e3311. Available from: https://doi.org/10.1002/cem.3311.

[34] Algamal ZY, Qasim MK, Lee MH, Ali HTM. High-dimensional QSAR/QSPR classification modeling based on improving pigeon optimization algorithm. *Chemometrics and Intelligent Laboratory Systems*. 2020; 206: 104170. Available from: https://doi.org/10.1016/j.chemolab.2020.104170.

[35] Al-Thanoon NA, Algamal ZY, Qasim OS. Improving meta-heuristic algorithms for feature selection in multiclass classification. In: Garcia FP, Jamil A, Hameed AA, Ortis A, Ramirez IS. (eds.) *Recent Trends and Advances in Artificial Intelligence*. Heidelberg: Springer; 2024. p.592-606. Available from: https://doi.org/10.1007/978-3-031-70924-1_45.

[36] AL-Taie FAY, Qasim OS, Algamal ZY. Improving kernel semi-parametric regression model based on a bat optimization algorithm. *AIP Conference Proceedings*. 2024; 3036: 040003. Available from: https://doi.org/10.1063/5.0202591.

[37] Almishlih ZA, Qasim OS, Algamal ZY. Design and evaluation of a new tent-shaped transfer function using the Polar Lights Optimizer algorithm for feature selection. *Informatyka, Automatyka, Pomiary w Gospodarce i Ochronie Środowiska [Informatics, Automatics and Measurements in Economy and Environmental Protection]*. 2025; 15(2): 27-31. Available from: https://doi.org/10.35784/iapgos.6802.

[38] Zhou X, Wu Z, Wang H. Elite opposition-based differential evolution for solving large-scale optimization problems and its implementation on GPU. In: *2012 13th International Conference on Parallel and Distributed Computing, Applications and Technologies*. Beijing, China: IEEE; 2012. Available from: https://doi.org/10.1109/PDCAT.2012.70.

[39] Wu X, Zhou Y, Lu Y. Elite opposition-based water wave optimization algorithm for global optimization. *Mathematical Problems in Engineering*. 2017; 11: 1-25. Available from: https://doi.org/10.1155/2017/3498363.

[40] Zhao R, Luo Q, Zhou Y. Elite opposition-based social spider optimization algorithm for global function optimization. *Algorithms*. 2017; 10(1): 9. Available from: https://doi.org/10.3390/a10010009.

[41] Huang K, Zhou Y, Wu X, Luo Q. A cuckoo search algorithm with elite opposition-based strategy. *Journal of Intelligent Systems*. 2015; 25(4): 567-593. Available from: https://doi.org/10.1515/jisys-2015-0041.

[42] Zhang S, Luo Q, Zhou Y. Hybrid grey wolf optimizer using elite opposition-based learning strategy and simplex method. *International Journal of Computational Intelligence and Applications*. 2017; 16(2): 1750012. Available from: https://doi.org/10.1142/S1469026817500122.

[43] Zhou Y, Wang R, Luo Q. Elite opposition-based flower pollination algorithm. *Neurocomputing*. 2016; 188: 294-310. Available from: https://doi.org/10.1016/j.neucom.2015.01.110.

[44] Tubishat M, Abushariah MAM, Idris N, Aljarah I. Improved whale optimization algorithm for feature selection in Arabic sentiment analysis. *Applied Intelligence*. 2019; 49(5): 1688-1707. Available from: https://doi.org/10.1007/s10489-018-1334-8.

[45] Chopra N, Mohsin Ansari M. Golden jackal optimization: A novel nature-inspired optimizer for engineering applications. *Expert Systems with Applications*. 2022; 198: 116924. Available from: https://doi.org/10.1016/j.eswa.2022.116924.

[46] Houssein EH, Abdelkareem DA, Emam MM, Hameed MA, Younan M. An efficient image segmentation method for skin cancer imaging using improved golden jackal optimization algorithm. *Computers in Biology and Medicine*. 2022; 149: 106075. Available from: https://doi.org/10.1016/j.compbiomed.2022.106075.

[47] Rezaie M, Karamnejadi Azar K, Kardan Sani A, Akbari E, Ghadimi N, Razmjooy N, et al. Model parameters estimation of the proton exchange membrane fuel cell by a Modified Golden Jackal Optimization. *Sustainable Energy Technologies and Assessments*. 2022; 53: 102657. Available from: https://doi.org/10.1016/j.seta.2022.102657.

[48] Mohapatra S, Mohapatra P. Fast random opposition-based learning Golden Jackal Optimization algorithm. *KnowledgeBased Systems*. 2023; 275: 110679. Available from: https://doi.org/10.1016/j.knosys.2023.110679.

[49] Devi RM, Premkumar M, Kiruthiga G, Sowmya R. IGJO: An improved golden jackel optimization algorithm using local escaping operator for feature selection problems. *Neural Processing Letters*. 2023; 55: 6443-6531. Available from: https://doi.org/10.1007/s11063-023-11146-y.

[50] Alharthi AM, Kadir DH, Al-Fakih AM, Algamal ZY, Al-Thanoon NA, Qasim MK. Improving golden jackel optimization algorithm: An application of chemical data classification. *Chemometrics and Intelligent Laboratory Systems*. 2024; 250: 105149. Available from: https://doi.org/10.1016/j.chemolab.2024.105149.

[51] Yang J, Xiong J, Chen YL, Yee PL, Ku CS, Babanezhad M. Improved golden jackal optimization for optimal allocation and scheduling of wind turbine and electric vehicles parking lots in electrical distribution network using rosenbrock's direct rotation strategy. *Mathematics*. 2023; 11(6): 1415. Available from: https://doi.org/10.3390/math11061415.

[52] Zhang K, Liu Y, Mei F, Sun G, Jin J. IBGJO: Improved binary golden jackal optimization with chaotic tent map and cosine similarity for feature selection. *Entropy*. 2023; 25(8): 1128. Available from: https://doi.org/10.3390/e25081128.

[53] Yuan P, Zhang T, Yao L, Lu Y, Zhuang W. A hybrid golden jackal optimization and golden sine algorithm with dynamic lens-imaging learning for global optimization problems. *Applied Sciences (Switzerland)*. 2022; 12(19): 9709. Available from: https://doi.org/10.3390/app12199709.

[54] Benachour S, Bendjeghaba O. Golden jackal algorithm for optimal size and location of distributed generation in unbalanced distribution networks. *Algerian Journal of Renewable Energy and Sustainable Development*. 2023; 5(1): 28-39. Available from: https://doi.org/10.46657/ajresd.2023.5.1.4.

[55] Tizhoosh HR. Opposition-based learning: A new scheme for machine intelligence. In: *International Conference on Computational Intelligence for Modelling, Control and Automation and International Conference on Intelligent Agents, Web Technologies and Internet Commerce (CIMCA-IAWTIC'06)*. Vienna, Austria: IEEE; 2005. Available from: https://doi.org/10.1109/CIMCA.2005.1631345.

[56] Elgamal ZM, Yasin NM, Sabri AQM, Sihwail R, Tubishat M, Jarrah H. Improved equilibrium optimization algorithm using elite opposition-based learning and new local search strategy for feature selection in medical datasets. *Computation*. 2021; 9(6): 68. Available from: https://doi.org/10.3390/computation9060068.

[57] Sihwail R, Omar K, Ariffin KAZ, Tubishat M. Improved harris hawks optimization using elite opposition-based learning and novel search mechanism for feature selection. *IEEE Access*. 2020; 8: 121127-121145. Available from: https://doi.org/10.1109/ACCESS.2020.3006473.

[58] Mahmood SW, Basheer GT, Algamal ZY. Quantitative structure-activity relationship modeling based on improving kernel ridge regression. *Journal of Chemometrics*. 2025; 39(5): e70027. Available from: https://doi.org/10.1002/cem.70027.

[59] Mahmood SW, Basheer GT, Algamal ZY. Improving kernel ridge regression for medical data classification based on meta-heuristic algorithms. *Kuwait Journal of Science*. 2025; 52(3): 100408. Available from: https://doi.org/10.1016/j.kjs.2025.100408.

[60] Mooney P. *Breast histopathology images*. Available from: https://wwwkagglecom/datasets/paultimothymooney/breast-histopathology-images [Accessed 27th June 2024].

[61] Singh MK, Chand S. Hybrid sigmoid activation function and transfer learning assisted breast cancer classification on histopathological images. *Multimedia Tools and Applications*. 2023; 83: 59043-59060. Available from: https://doi.org/10.1007/s11042-023-17808-2.